Partial Differential Equations in Applied Mathematics 4 (2021) 100184

Contents lists available at ScienceDirect

Partial Differential Equations in Applied Mathematics

journal homepage: www.elsevier.com/locate/padiff

Significance of variable electrical conductivity on non-Newtonian fluid flow between two vertical plates in the coexistence of Arrhenius energy and exothermic chemical reaction

Adebowale Martins Obalalu [a,*], Olusegun Adebayo Ajala [c], Adeshina Taofeeq Adeosun [b], Akintayo Oladimeji Akindele [c], Olayinka Akeem Oladapo [c], Olatunbosun Akintayo Olajide [c], Adegbite Peter [c]

[a] Department of Statistics and Mathematical Sciences, Kwara State University, Malete, Nigeria
[b] Department of Mathematics University of Ilorin, Ilorin, Nigeria
[c] Department of Pure and Applied Mathematics, Ladoke Akintola University of Technology, Ogbomoso, Nigeria

ARTICLE INFO

Keywords:
Magnetohydrodynamics fluid
Rheological Casson fluid
Arrhenius energy and exothermic chemical reaction

ABSTRACT

The present study is designed to model the combustible materials of two vertical plates with Arrhenius energy and exothermic chemical reaction. The magnetohydrodynamics fluid is considered to experience an exothermic chemical reaction inside the channel. Additional effects incorporated to the novelty of the model are the rheological Casson fluid term and the variable electrical conductivity. The model has transformed appropriately to its dimensionless form using similarity renovation and the Solution is numerically obtained using the Chebyshev collocation scheme. The influences of controlling parameters on the fluid velocity, temperature, concentration, and heat transfer rate are analyzed using graph and quantitatively discussed. Analyses reveal that the activation energy declines the fluid velocity, while the existence of the variable electrical conductivity parameter has the opposite effect. The heat transfer rate is enhanced with higher values of concentration buoyancy (Gc) and variable electrical conductivity parameter. Moreover, the non-Newtonian Casson fluid parameter shows a solid characteristic when yield stress is more than the shear stress. Thermal and chemical engineering, as well as service-worthiness of industrial products, will benefit from the findings of this study.

1. Introduction

Chemical reaction modifies the composition quantity of chemical components. When the chemical relationship between atoms is disrupted, only the internal structure is transferred. The chemical reaction is among the most important factors that influence the reaction rate. The chemical reaction plays an important role in enhancing traditional fluid heat transfer. In the manufacturing industry, major engineering activities such as drying, temperature, and moisture distribution can be carried out using heat and mass transfer due to chemical reactions.[1] For most chemical reaction cases, the response rate is influenced by the reactant concentration. A chemical reaction occurs when the rate of reaction is directly proportional to the concentration of the reactant. There are two kinds of chemical reactions: exothermic and endothermic. An exothermic reaction is described as a heat-releasing reaction that has a significant negative enthalpy modification (see Fig. 1).[2] However, many chemical reactions produce heat, light, or sound as a byproduct. This is an example of an exothermic reaction. Exothermic reactions release energy in the form of heat into the surrounding environment. Endothermic is called chemical reactions which absorb (or use) energy. However, the thermite reaction, iron rusting, burning sugar–water freezing, and combustion process are examples exothermic. More energy is absorbed by endothermic reactions when reactant links are broken as they are released when new bonds form in the products (see Fig. 1).

However, when the heat produced exceeds, the heat lost to the atmosphere, and the exothermic fuel reaction might result in a combustible reaction. To ensure the safety of life and property, thermal stability and thermal effect appear to be essential. In a reactive system, the activation energy is essential energy needed for chemical species atoms or molecules to start a reaction. This model includes the active energy that most researchers have not considered in earlier studies.[3–6] A numerical study of Chemical reactions on non-Newtonian on squeeze flow with slip condition was studied by Ref. 7. The effect of Arrhenius energy on the hydromagnetic fluid of two-dimensional electrically conducting with a porous material was the numerical study by Ref. 8. The 2D stratified flow of an Oldroyd-B fluid with chemical reaction: an application of non-Fourier heat flux theory was study by Ref. 9

* Corresponding author.
E-mail address: adebowale.obalalu17@kwasu.edu.ng (A.M. Obalalu).

https://doi.org/10.1016/j.padiff.2021.100184
Received 16 August 2021; Received in revised form 2 October 2021; Accepted 22 October 2021

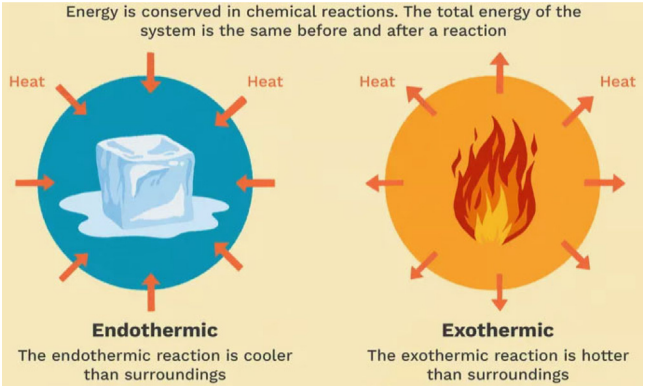

Fig. 1. Chemical reactions with exothermic and endothermic.

In recent years, technological innovation has considerably contributed to the growing demand for non-Newtonian fluids. These fluids have various rheological features, which makes them more relevant to chemical, biomedical sciences chemical engineering, pharmaceutical, and then the Newtonian fluids. The relationship between the local strain rate and the viscous stresses is caused by Newtonian liquid dynamics. This implies that the connection between viscous stresses caused by flow is not time-dependent and linear. However, the non-Newtonian fluids are drugs, blood, toothpaste, ketchup, cosmetics, food, soap. Moreover, there are three types of non-Newtonian liquids such as time-independent, viscoelastic, and time-dependent. Also, the viscosity of non-Newtonian fluids depends on the temperature, time, and shear rate. Therefore, the Non-Newtonian fluids, which depend on time, are fluids in which stress only influences the shear rate at a specific moment. In addition, among these non-Newtonian fluids fluid models. The Casson fluid (CF) is one of the most widely utilized viscoelastic non-Newtonian materials. In various fields, including scientific, engineering, and food processing, CF has gained considerable interest. Examples of common CF-properties are Jelly, Oil, Paint, and honey.[1] However, at low shear stress, the non-Newtonian CF acts as a solid elastic; But it acts like a Newtonian CF at critical stress The pioneering work regarding the CF model was the work of Casson which defines the pigment–oil suspension prediction flow. Casson's work[10] laid the groundwork for non-Newtonian fluid flow investigation. However, the analysis predicted the pigment–oil suspension's flow behavior. Physically, the yield shear stress must be greater than the magnetohydrodynamic shearing property of the non-Newtonian Cf. In regards to this, the work of Obalalu[11] studies the non-Newtonian CF of hydrodynamic unsteady squeezed flow in presence of variable thermophysical properties. Since then various scientists[12–18] have studied the CF model's usefulness, recently, A mathematical model was established by Gbadeyan et al.[19] to analyze the performance of CF and variable transport properties on a Casson nanofluid flow. Mukhopadhyay et al.[20] Studied the effect of CF with thermal convection to investigate the performance of heat and mass transfer in an exponentially stretching permeable surface. Obalalu[21] exhibited that the utilizing of rheological CF to enhance the behavior of thermodynamics for better cooling. Hari and Harshad[14] discussed the Importance of Radiative Casson fluid and the chemical reaction of Hydromagnetic flow passing through an oscillating vertical plate. A semi-analytical study has been performed by Obalalu[22] in examining the rheological Casson fluid on hydrodynamic Natural Convective flow with a porous material. A mathematical and computational framework for heat transfer analysis of ferromagnetic non-Newtonian liquid subjected to heterogeneous and homogeneous reactions were study by Ref. 23.

Magnetic technologies are becoming more attractive in industries due to a variety of applications in biomaterials for wound treatment,[24] gastrointestinal drugs,[25] sterilizing devices,[26] and other related fields. However, magnetic fields are known to be utilized for the regulation of electrically conducting that can be orchestrated to accomplish the intended results in applications. Since the pioneering work[27] studies related to the magnetohydrodynamics (MHD) is One of the important areas of development in modern scientific research and engineering problems is magnetohydrodynamics which can also be considered as a fluid mechanics subdiscipline dealing with the mutual interactions between an externally imposed magnetic field and the flows of fluids that conduct electricity.[28] However, the study of magnetic properties and compliance of electrically conducting liquids is magnetic hydrodynamics. Some more interesting applications included magnetic levitation chilling and MHD molten metal is in the field of metallurgy. This kind of difficulty also occurs during operating in micro-electronic devices and electronic packages. Hartmann and Lazarus[1] were the first to investigate the modern MHD flow in a laboratory. Akbar et al.[29] revealed that the utilizing of magnetic field and Convective heating improved the performance of the heat transfer fluids. While Obalalu et al.[30] scrutinized the magnetic field and heat generation effect on unsteady vertical hydrodynamic flow through a porous channel with convective boundary conditions. A numerical study has been performed by Ref. 31 in investigating the viscous dissipation and higher-order chemical reactions on magnetic hydrodynamics nanofluid flow. Eegunjobi and Makinde[32] showed that utilizing the magnetic field as the fundamental fluid improved viscous MHD channel flow. Furthermore, Due to its high electrical conductivity, which is a function of the temperature, and metal, therefore the velocity field and the distribution of temperature of liquid metals are modified in the presence of a transverse magnetic field, which changes in inversity in terms of temperature. Therefore, the application of the electric field is one of the most successful ways to improve heat transmission. Consequently, the temperature-dependent electrical conductivity becomes a topic of investigation the this current studies. However, we are interested in knowing if temperature-dependent electrical conductivity have a significant effect on flow and fluid properties of two vertical plates.The Simulation of revised nanofluid model in the stagnation region of cross fluid by expanding–contracting cylinder were investigated by Ref. 33. The Thermally radiative stagnation point flow of Maxwell nanofluid due to unsteady convectively heated stretched surface were investigated by Ref. 34. Entropy optimized Darcy–Forchheimer nanofluid (silicon dioxide, molybdenum disulfide) subject to temperature dependent viscosity were investigated by Ref. 29.

Based on the discussions above, the objective of this current exploration focuses on hydrodynamics non-Newtonian flow of combustible materials between two vertical plates. The analysis of variable electrical conductivity is included to explore the flow and heat interaction. This analysis is inspired by the high demand for diverse industrial working fluids and previous presentations on the importance of Arrhenius energy and exothermic chemical reaction to biotechnology, thermal sciences, chemical engineering, food processing, and others. To the best of our knowledge, no investigation on the mentioned issues has so far been reported. The governing equations of the flow are solved numerically, and the velocity, temperature, heat transfer rate figures are captured to have requisite information of the flow and heat transfer. The rest of the article is organized as follows. The mathematical formulation of the problem is presented in the next section. Section 3 deals with the concept of Chebyshev-based collocation method and its application in solving the present nonlinear boundary value problems. In Section 4, the obtained numerical results are presented graphically and discussed. Concluding remarks are given in the last section

2. Mathematical model

The hydromagnetic non-Newtonian reacting fluid and non-linear convection flow filled with homogeneous porous materials between two vertical plates is studied in the presence of induced electric field and imposed magnetic field (see Fig. 2). The x-axis is parallel to the

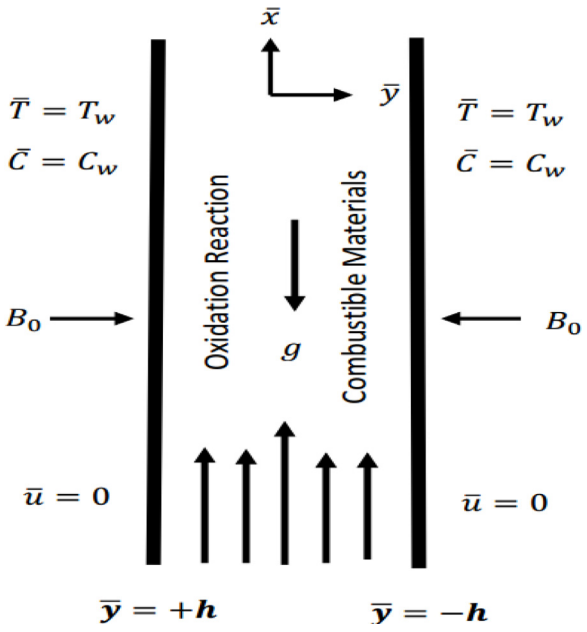

Fig. 2. The physical geometry of the flow.

channel, and the y axis is perpendicular to it. The fluid temperature T_w, and concentration C_w are applied to the channel walls at a constant temperature. From this assumption. The flow is driven by, temperature, concentration gradients, and constant pressure.[2]

The modified governing equations are

$$\left(1+\frac{1}{\beta}\right)\mu\frac{d^2\bar{u}}{d\bar{y}^2}+g\rho\beta_{T_0}(\bar{T}-T_0)+g\rho\beta_{T_1}(\bar{T}-T_0)^2 + g\rho\beta_{C_0}(\bar{C}-C_0)+g\rho\beta_{C_1}(\bar{C}-C_0)^2-\sigma B_0^2u-\frac{dP}{dx}-\left(1+\frac{1}{\beta}\right)\frac{\mu}{K}\bar{u}=0 \tag{2.1}$$

$$\frac{d^2\bar{T}}{d\bar{y}^2}+\frac{QA(\bar{C}-C_0)}{k_T}exp\left(-\frac{E}{R\bar{T}}\right)+\left(1+\frac{1}{\beta}\right)\frac{\mu}{k_T}\left(\frac{d\bar{u}}{d\bar{y}}\right)^2 + \left(1+\frac{1}{\beta}\right)\frac{\mu}{k_TK}\bar{u}^2+\frac{\sigma B_0^2}{k_T}\bar{u}^2=0 \tag{2.2}$$

$$\frac{d^2\bar{C}}{d\bar{y}^2}-\frac{A(\bar{C}-C_0)}{D}exp\left(-\frac{E}{R\bar{T}}\right)=0 \tag{2.3}$$

Subjected to:

$$\left.\begin{aligned}&\bar{u}=0,\bar{T}=T_w,\bar{C}=C_w,at\ \bar{y}=-h\\&\bar{u}=0,\bar{T}=T_w,\bar{C}=C_w,at\ \bar{y}=h\end{aligned}\right\} \tag{2.4}$$

In the literature, there are few kinds of electrical conductivity differences. We choose the one that is absolute for liquid, which is as follows:

$$\frac{1}{\sigma}=\frac{1}{\sigma'}\left[(1+\varepsilon'(\mathrm{T}-\mathrm{T}_\infty))\right] \tag{2.5}$$

Where σ is the surface temperature electrical conductivity and ε' is a constant dependent on the fluid's electrical conductivity. We present the non-dimensional variation parameter of electrical conductivity

$$\varepsilon=\varepsilon'\left(\mathrm{T_w}-\mathrm{T_\infty}\right) \tag{2.6}$$

Substituting (2.6) and (2.7) into (2.5) yields:

$$\sigma'=\frac{\sigma 1}{1+\varepsilon\theta} \tag{2.7}$$

We introduce the following non-dimensional quantities:

$$Gr=\frac{\rho\beta_{T_0}gh^2RT_0^2}{\mu UME},y=\frac{\bar{y}}{h},\phi=\frac{\bar{C}-C_0}{C_w-C_0},u=\frac{\bar{u}}{UM},M=\frac{h^2dp}{\mu Udx}, \tag{2.8}$$

$$\sigma_1=\frac{\beta_{T_1}RT_0^2}{\beta_{T_0}E},\lambda=\frac{QEAh^2(C_w-C_0)}{RT_0^2k_T}exp\left(-\frac{E}{RT_0}\right),\epsilon=\frac{RT_0}{E}$$

$$\sigma_2=\frac{\beta_{C_1}(C_w-C_0)}{\beta_{C_0}E},\theta_w=\frac{E(\bar{T}_w-T_0)}{RT_0^2},$$

$$Kr=\frac{k_TRT_0^2}{QED(C_w-C_0)},\delta=\frac{U^2\mu M^2}{QAh^2(C_w-C_0)}exp\left(-\frac{E}{RT_0}\right),$$

$$\beta=\sqrt{\frac{1}{Da}},Da=\frac{K}{h^2},\mathrm{Ha}^2=\frac{\sigma B_0^2h^2}{\mu},Gc=\frac{\rho gh^2\beta_{C_0}(C_w-C_0)}{\mu UM},$$

$$\theta=\frac{E(\bar{T}-T_0)}{RT_0^2}$$

where σ_1 and σ_2 is nonlinear thermal and concentration convection parameter, P permeability of the porous medium, Gr thermal buoyancy parameter, Ha Hartmann number, D — reactant diffusivity, λ Frank–Kamenetski parameter, β_{T_0} linear volumetric, C_w reactant concentration wall, T_w wall temperature, δ viscous heating parameter, Kr reactant concentration consumption rate parameter, $\bar{T}$ — absolute temperature, $\bar{C}$ reactant concentration, μ — fluid dynamic viscosity, θ_w wall temperature parameter, β porous medium parameter, Kr wall temperature parameter, σ electrical conductivity, ϵ activation energy parameter, c Casson parameter. $\bar{u}$ — axial velocity, ε variable electrical conductivity parameter. Using Eqs. (2.7) and (2.8), Eqs. (2.1) and (2.4) reduces to:

$$1+\left(1+\frac{1}{\beta}\right)\frac{d^2u}{dy^2}+Gr\left(\theta+\sigma_1\theta^2\right)+Gc\left(\phi+\sigma_2\phi^2\right) - \left(1+\frac{1}{\beta}\right)\beta^2u-\frac{\mathrm{Ha}^2}{(1+\varepsilon\theta)}u=0 \tag{2.9}$$

$$\frac{d^2\theta}{dy^2}+\lambda\left[\phi\ exp\left(\frac{\theta}{1+\epsilon\theta}\right)+\delta\left(\left(1+\frac{1}{\beta}\right)\left(\frac{du}{dy}\right)^2 + \left(1+\frac{1}{\beta}\right)\beta^2u^2+\frac{\mathrm{Ha}^2}{(1+\varepsilon\theta)}u^2\right)\right]=0 \tag{2.10}$$

$$\frac{d^2\phi}{dy^2}-Kr\ \lambda\ \phi\ exp\left(\frac{\theta}{1+\epsilon\theta}\right)=0 \tag{2.11}$$

$$\left.\begin{aligned}&u=0,\theta=\theta_w,\phi=1,\ at\ y=-1\\&u=0,\theta=\theta_w,\phi=1,\ at\ y=1\end{aligned}\right\} \tag{2.12}$$

The term, $exp\left(\frac{\theta}{1+\epsilon\theta}\right)$, in Eqs. (2.10) and (2.11) is approximated as

$$exp\left(\frac{\theta}{1+\epsilon\theta}\right)\approx 1+\theta+\theta^3\left(\epsilon^2-\epsilon+\frac{1}{6}\right)+\theta^2\left(\frac{1}{2}-\epsilon\right) \tag{2.13}$$

Therefore, Eqs. (2.10) and (2.11) become

$$\frac{d^2\theta}{dy^2}+\lambda\left[\phi\left(1+\theta+\theta^3\left(\epsilon^2-\epsilon+\frac{1}{6}\right)+\theta^2\left(\frac{1}{2}-\epsilon\right)\right) + \delta\left(\left(1+\frac{1}{\beta}\right)\left(\frac{du}{dy}\right)^2+\left(1+\frac{1}{\beta}\right)\beta^2u^2+\frac{\mathrm{Ha}^2}{(1+\varepsilon\theta)}u^2\right)\right]=0 \tag{2.14}$$

$$\frac{d^2\phi}{dy^2}-Kr\,\lambda\phi\left(1+\theta+\theta^2\left(\frac{1}{2}-\epsilon\right)+\theta^3\left(\epsilon^2-\epsilon+\frac{1}{6}\right)\right)=0 \tag{2.15}$$

The rate of heat transfer across the reactive surface wall is given by

$$-\frac{d}{dy}\theta(1)=Nu. \tag{2.16}$$

3. Numerical solution

3.1. A summary of the Chebyshev collocation scheme (CCS)

The solution of the equations systems in closed form of Eqs. (2.9)–(2.11) turns out to be a difficult task in terms of non-linearity. Consequently, because of their vast capacity for managing linear and nonlinear equations systems, a numerical methodology of the Chebyshev-based collocation method was developed. The method is based on the

expansion with the effectiveness of the Chebyshev polynomial. At first, we consider a trial solution that depends on the unknown coefficient to the Chebyshev base function, also by applying the trial solution on the boundary condition, then the use of a collocation approach as the control system to generate the residual error is minimize closed to zero.

3.2. Application of CCS

We assume $u(y), \theta(y)$ and $\phi(y)$ as Chebyshev base trial functions, defined by

$$u(y) = \sum_{k=0}^{R} a_i T_i(2y-1), \quad \theta(\eta) = \sum_{k=0}^{R} b_i T_i(2y-1) \text{ and } \phi(\eta) = \sum_{k=0}^{R} c_i T_i(2y-1) \tag{3.17}$$

The constants to be obtained are a_i, b_i and c_i, and $T_i(2y-1)$ is the shifted Chebyshev function. Also substituting Eq. (3.17) into the governing equation (2.9) (2.10) and (2.11) produce

$$D_\theta = \theta_{y,2} + \lambda \left[\phi\left(1+\theta+\theta_y^3\left(\epsilon^2-\epsilon+\frac{1}{6}\right)+\theta_y^2\left(\frac{1}{2}-\epsilon\right)\right)\right. \tag{3.18}$$
$$\left. + \delta\left(\left(1+\frac{1}{\beta}\right)\theta_y^2 + \left(1+\frac{1}{\beta}\right)\beta^2 u^2 + \frac{\mathrm{Ha}^2}{(1+\epsilon\theta)}u^2\right)\right] = 0$$

$$D_\phi = \phi_y^2 - Kr\,\lambda\phi\left(1+\theta+\theta_y^2\left(\frac{1}{2}-\epsilon\right)+\theta_y^3\left(\epsilon^2-\epsilon+\frac{1}{6}\right)\right) = 0 \tag{3.19}$$

With boundary conditions

$$[u=0, \theta=\theta_w, \phi=1, \ at\ y=-1]_{y=0,} \tag{3.20}$$
$$[u=0, \theta=\theta_w, \phi=1, \ at\ y=1]_{y=0,}$$

In the same manner, Eq. (3.17) is substituted with Eqs. (2.9) (2.10) and (2.11) to produce residues $R_u(\eta, a_i)$, $R_\theta(\eta, a_i, b_i)$ and $R_\phi(a_i, d_l, \eta)$. As a result, the residues are reduced using the collocation method, as shown below.

$$\int_{-1}^{1} R_u \delta(y-y_j)\,dy = R_u(\eta_j, a_i, b_i, c_i) = 0, \qquad for\ j = 1, 2, \ldots, N-1 \tag{3.21}$$

$$\int_{-1}^{1} R_\theta \delta(y-y_j)\,dy = R_\theta(\eta_j, a_i, b_i, c_i) = 0, \qquad for\ j = 1, 2, \ldots, N-1 \tag{3.22}$$

$$\int_{-1}^{1} R_\phi \delta(y-y_j)\,dy = R_\phi(\eta_j, a_i, b_i, c_i) = 0, \qquad for\ j = 1, 2, \ldots, N-3 \tag{3.23}$$

where $\eta_j = \frac{1}{2}\left(1 - cos\left(\frac{j\pi}{N}\right)\right)$. Eqs. (3.21)–(3.23) is therefore producing an algebraic equation system of 2N + 2 with unknown coefficients (a_i, b_i, c_i). By using Mathematical Symbolic Package MATHEMATICA 11.3, the equations are solved by the Newton technique to obtain constant coeffective values. Table 1 shows the convergence of CCS for various approximation order.

4. Validation, computational results, and discussion

This segment is designed to address the behavior of the fluid parameters on the fluid velocity, temperature, concentration profile, and heat transfer rate through plots and table for magnetohydrodynamics reactive fluid. Unless otherwise mentioned, the following default parametric values are used in this analysis: $\epsilon = 0.5$, $\beta = 1, \sigma_2 = 1, Gc = 1, Kr = 0.1$ Ha $= 1$, c $= 0.1, Gr = 1, \lambda = 0.5, \sigma_1 = 1, \delta = 0.3$, and $\theta_w = 0.1$, and Unless otherwise indicated as default parameters. The values of velocity, temperature, concentration for the problem were compared with previously published results to ascertain the accuracy of the current method. However, our result agrees with the previous work (see Table 2). The inference of reaction rate parameter (λ) is observed

Table 1
CCS solutions in various approximation orders of Convergence when $\epsilon = 0.5$, $\beta = 1, \sigma_2 = 1, Gc = 1, Kr = 0.1$ Ha $= 1, c = 0.1, Gr = 1, \lambda = 0.5, \sigma_1 = 1, \delta = 0.3, c = 0.2, \varepsilon = 1$ *and* $\theta_w = 0.1$.

Number of iteration (N)	u	θ	ϕ
4	3.054620	0.233124	0.358571
6	3.004633	0.180744	0.297306
8	3.002122	0.98752	0.06982
10	3.001933	0.987525	0.06982
12	3.001933	0.98752	0.06982
14	3.001933	0.180557	0.296766
16	3.001933	0.180557	0.296766
20	3.001933	0.180557	0.296766
24	3.001933	0.180557	0.296766
30	3.001933	0.180557	0.296766

Table 2
Comparison of velocity, temperature, concentration for different values of y when: $\epsilon = 0.5$, $\beta = 1, \sigma_2 = 1, Gc = 1, Kr = 0.1$ Ha $= 1, c = 0.1, Gr = 1, \lambda = 0.5, \sigma_1 = 1, \delta = 0.3, c = \infty, \varepsilon = 0$ *and* $\theta_w = 0.1$.

y	u		θ		ϕ	
	CCM	0HAM[8]	CCM	0HAM[8]	CCM	0HAM[8]
−1.00	0.000000	0.000000	0.100000	0.100000	1.000000	1.000000
−0.75	0.477790	0.477790	0.129493	0.129493	0.997476	0.997476
−0.50	0.795743	0.795743	0.150111	0.150111	0.995661	0.995661
−0.25	0.977544	0.977544	0.162382	0.162382	0.994566	0.994566
0.00	1.036685	1.036685	0.166463	0.166463	0.994200	0.994200
0.25	0.977544	0.977544	0.162382	0.162382	0.994566	0.994566
0.50	0.795743	0.795743	0.150111	0.150111	0.995661	0.995661
0.75	0.477790	0.477790	0.129493	0.129493	0.997476	0.997476
1.00	0.000000	0.000000	0.100000	0.100000	1.000000	1.000000

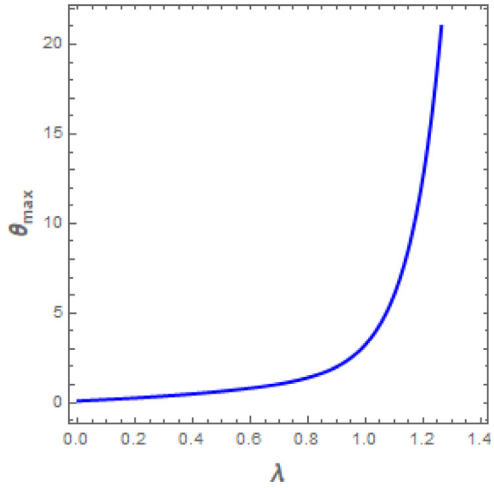

Fig. 3. Display the Temperature's blow-up for large values of reaction rate parameter λ.

in Temperature's blow-up (see Fig. 3). The graphic shows that the high values of λ parameter cause a thermal explosion (see Fig. 3).

The effect of Casson Fluid (CF) parameter (c) on velocity profile is demonstrated in Fig. 4(a). It was observed in this figure that the fluid flow increases with the mounting CF parameter. Physically, The Casson rheological behaves like a fluid due to its plastic dynamic viscosity, which has a strong effect on yield stress.[16] It also found that the Casson rheological increase the reaction of the non-Newtonian fluid. This means that the pure fluid acts in the same way as Newtonian fluid. On contrary, the CF parameter decreases the fluid temperature. The effect of Hartmann number (Ha) on velocity and temperature profile is elaborated in Fig. 4 (b, and c). The figure also found that an increment in the Hartmann number (Ha) reduced the velocity flow. Physically, A magnetic field is occurred in an electrically conducting fluid and

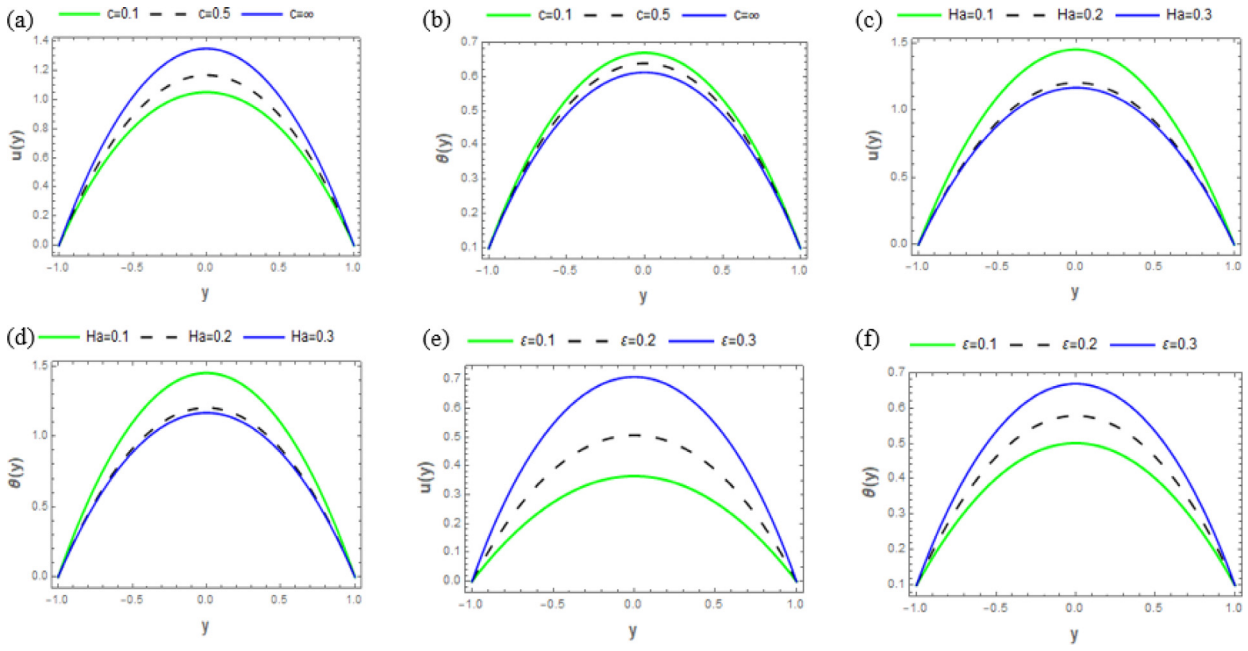

Fig. 4. Impact of Casson Fluid (CF) parameter (c), Hartmann number (Ha), and variable electrical conductivity (ε) on u(y), θ(y) and ϕ(y).

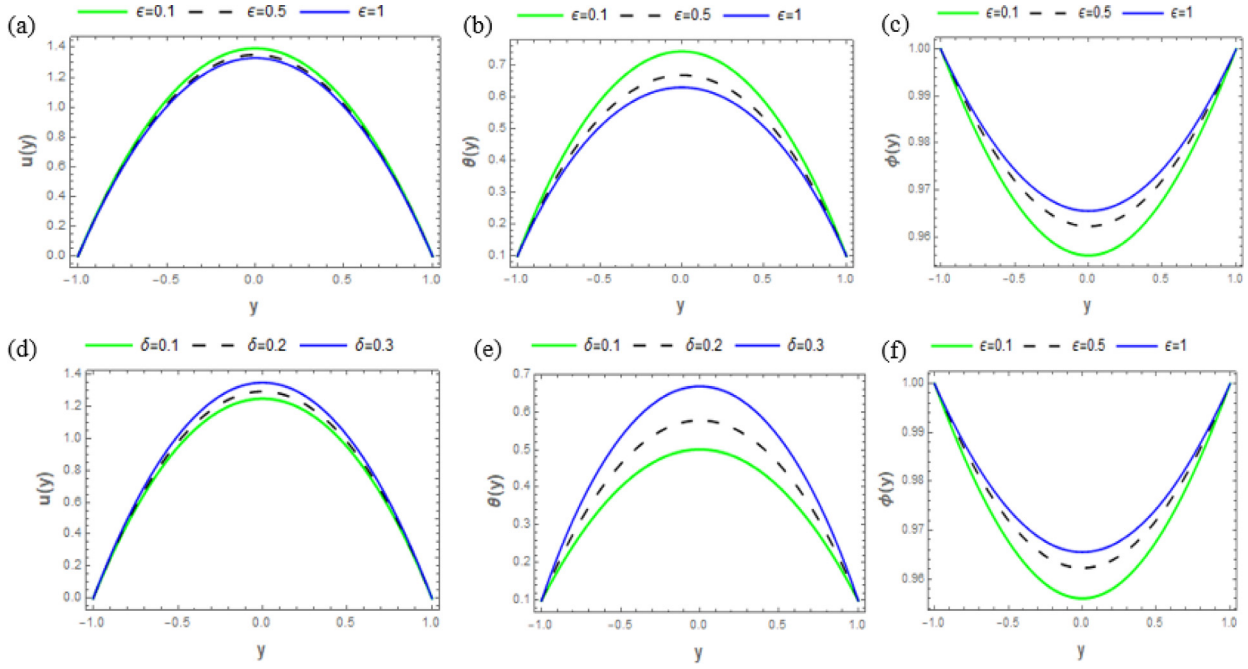

Fig. 5. Effect of activation energy (ϵ) and viscous heating parameter (δ) on $u(y), \theta(y)$ *and* $\phi(y)$.

adds a retarding body force that transversally reacts in the path of the applied magnetics force. With the applied magnetics force, the magnetohydrodynamic drag force slows down the motion of the fluid. This outcome has an important impact on numerous industrial applications, for solidification procedures like casting and semiconductor applications for single crystal growth. These claims provide significant implications on quality control for the product when the liquids have solidification, the liquid flow, and turbulence exist in the solidifying fluid pool. In solidifying systems, the technique of magnetic fields has been used well to monitor melt convection. The mounting parameter of the magnetic field has a contrary impact on temperatures profile (The Lorentz heating servers a resistive nature to the system fluid flow, however, the Lorentz heating is used as an extra source of heat within the channel. From Fig. 4(e), it was observed that the effect of variable electric conductivity Improves the fluid flow. The explanation is that the Lorentz force increasing due to the electrical field which serves as an accelerating force that lowering friction resistance. In addition, the electrical conductivity acts as an accelerating force that raises the thermal temperature. The effect of variable electrical conductivity (ε) parameter corresponds to the higher temperature in the channel. The increment of the temperature is characterized by the existence of Joule heating (or Lorentz heating) in the energy equation. Hence The electrical conductivity therefore serves as the heat source for the flow system (see Fig. 4(f)).

The effect of the activation energy (ϵ) is observed in velocity, temperature, and concentration profile is elaborated in Fig. 5 (a, b,

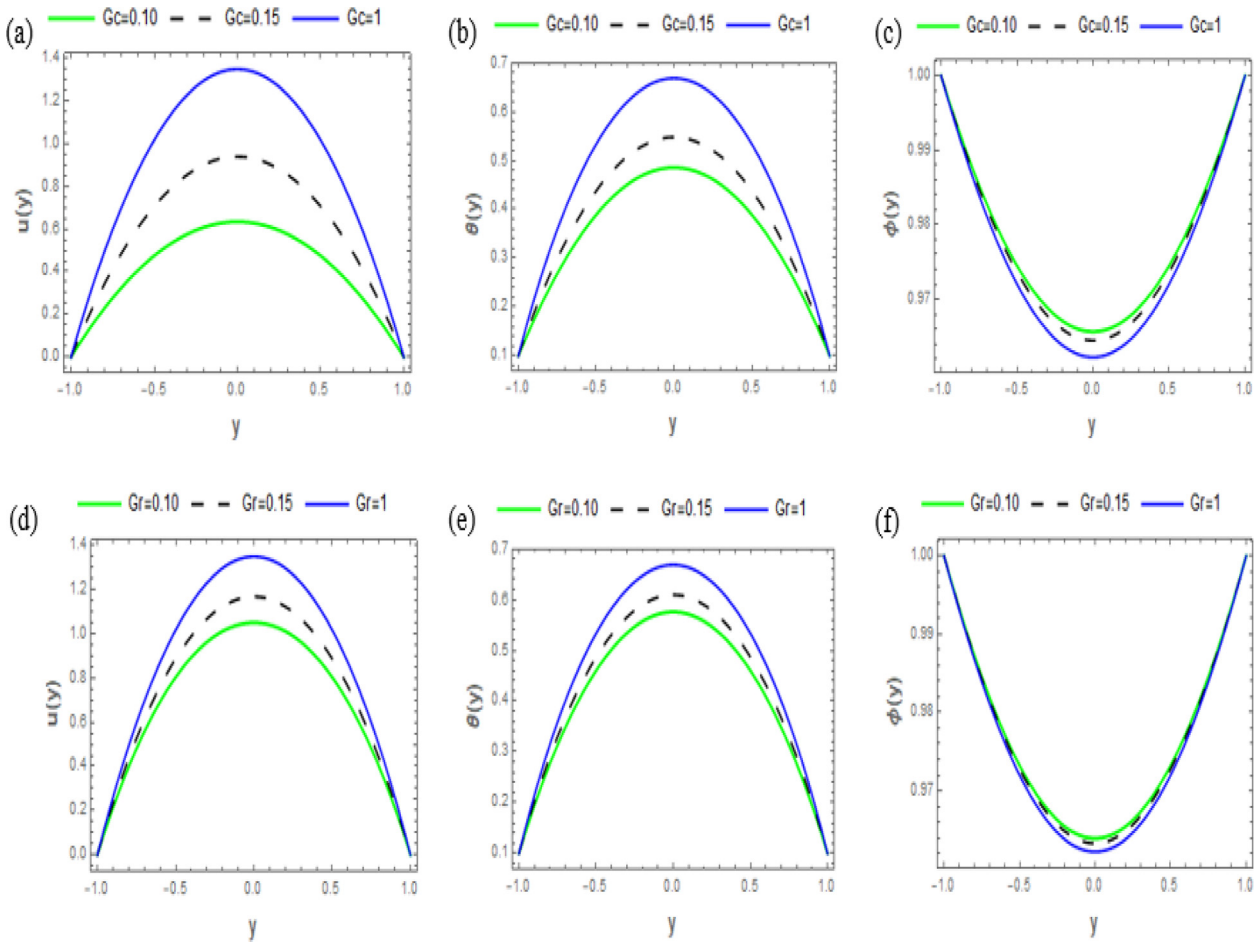

Fig. 6. Effect of concentration buoyancy (Gc) and thermal buoyancy (Gr) on $u(y), \theta(y)$ *and* $\phi(y)$.

c). As can be seen in the graph, an increment in activation energy parameter reduces the fluid flow and thermal profile inside the flow channel, whereas the concentration profile improved with an increased activation energy parameter. The explanation is that the $\exp\left(\frac{\theta}{1+\epsilon\theta}\right)$ function in Eqs. (2.9) and (2.10) reduce as the activation energy increase. Consequently the $\exp\left(\frac{\theta}{1+\epsilon\theta}\right)$ the function indicates the heat source term; therefore, the activation energy parameter decreases the fluid flow together with the thermal profile. Also, the concentration profile increased as the activation energy parameter increases. The explanation is that the function $\exp\left(\frac{\theta}{1+\epsilon\theta}\right)$ is subtracted from (2.11) thereby causing the reactant concentration profile to be enhanced. Fig. 5 (d, e, f) reveals the impact of the viscous heating parameter (δ) on fluid flow, thermal, and concentration profile. An increment in the δ leads to a reduction in the frictional forces and hence a decrease in flow resistance. This behavior can be seen in Fig. 5(d). The strength of the viscous heating sources in energy equations increases as fluid speed increases, resulting in a higher fluid temperature see (Fig. 5 e). From Fig. 5(e). The heat generated by viscous heating caused the reactant concentration to migrate into the wall, resulting in a reduction in the concentration profile.

Fig. 6(d, e, and f): Exhibit the impact of thermal buoyancy (Gr) on fluid flow, thermal, and concentration profile. These figures clearly show that the higher values of Gr enhance the fluid flow and thermal profile, while the concentration profile is decreased. The effect of Gr on the Casson velocity fluid is crucial due to the improvement in velocity profile, i.e., the stronger the buoyancy force, the higher the fluid motion. This is because the heat source term in the velocity equation indicates the thermal buoyance term. However, the fluid speed enhances the viscous heating sources in the temperature equation and leads to an improvement in thermal profile (see Fig. 6b). In addition, the concentration profile is depressed due to an increment in fluid temperature. Therefore, the effect of thermal buoyancy caused an exothermic chemical reaction to occur and decreases the concentration of the reactants (see Fig. 6c). Further, the greater values of concentration buoyancy parameter elevate the fluid flow and thermal profile, whereas the opposite effect is found in the reactant concentration profile. This behavior can be seen in Fig. 6(a, b, and c). This is the outcome of the logical reasoning used to justify in Fig. 6(a, b, and c)

Fig. 7 (a b, and c) shows the impact of reactant concentration consumption rate parameter (Kr) on fluid flow, thermal, and concentration profile for. As observed, the exothermic chemical reaction and internal heat generated decreased with higher values of Kr. Hence, the chemical reaction decreases the fluid motion. The variations of Frank–Kamenetski (reaction rate parameter, λ) on fluid flow, thermal, and concentration profile are demonstrated in Fig. 7 Fig. 6(d, e, and f), we observed that the velocity and fluid temperature reduce with a Frank–Kamenetski (reaction rate parameter, λ). With higher values of (reaction rate parameter, λ) substantial improvements in the exothermic chemical reaction and significantly increased the thermal profile together with the Temperature's blow up (see Fig. 3). Physically, the exothermic chemical reactions lead to strengthening in the internal heat generation due to higher values of (reaction rate parameter, λ). Meanwhile, the speeds of exothermic chemical reactions control internal heat production. In addition, the flow is dragged thereby causes a reduction in the concentration profile.

From Fig. 8, The heat transfer rate is enhanced with higher values of concentration buoyancy (Gc) and variable electrical conductivity (ε), also an increment in Hartmann number (Ha), reactant concentration

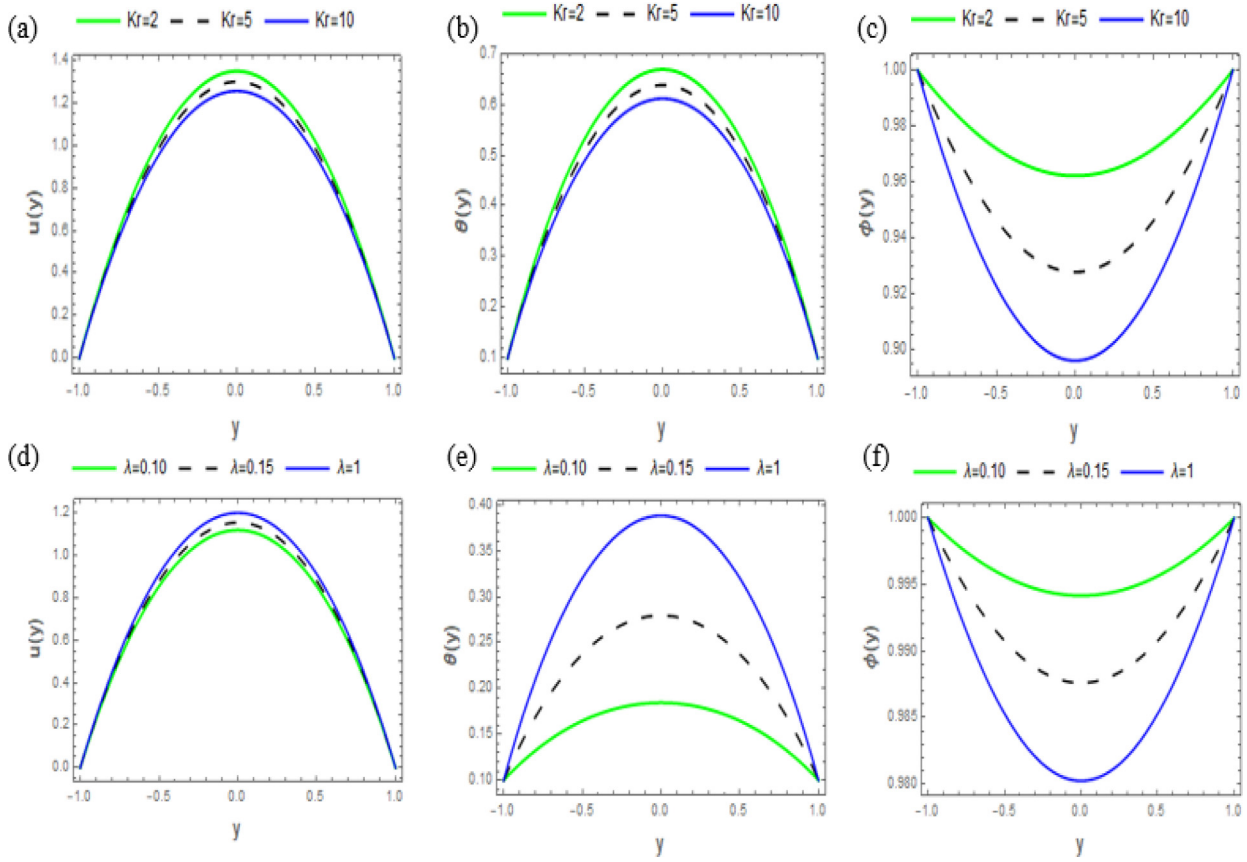

Fig. 7. Impact of reactant concentration consumption rate parameter (Kr) and reaction rate parameter, λ, concentration buoyancy (Gc) on $u(y), \theta(y)$ *and* $\phi(y)$.

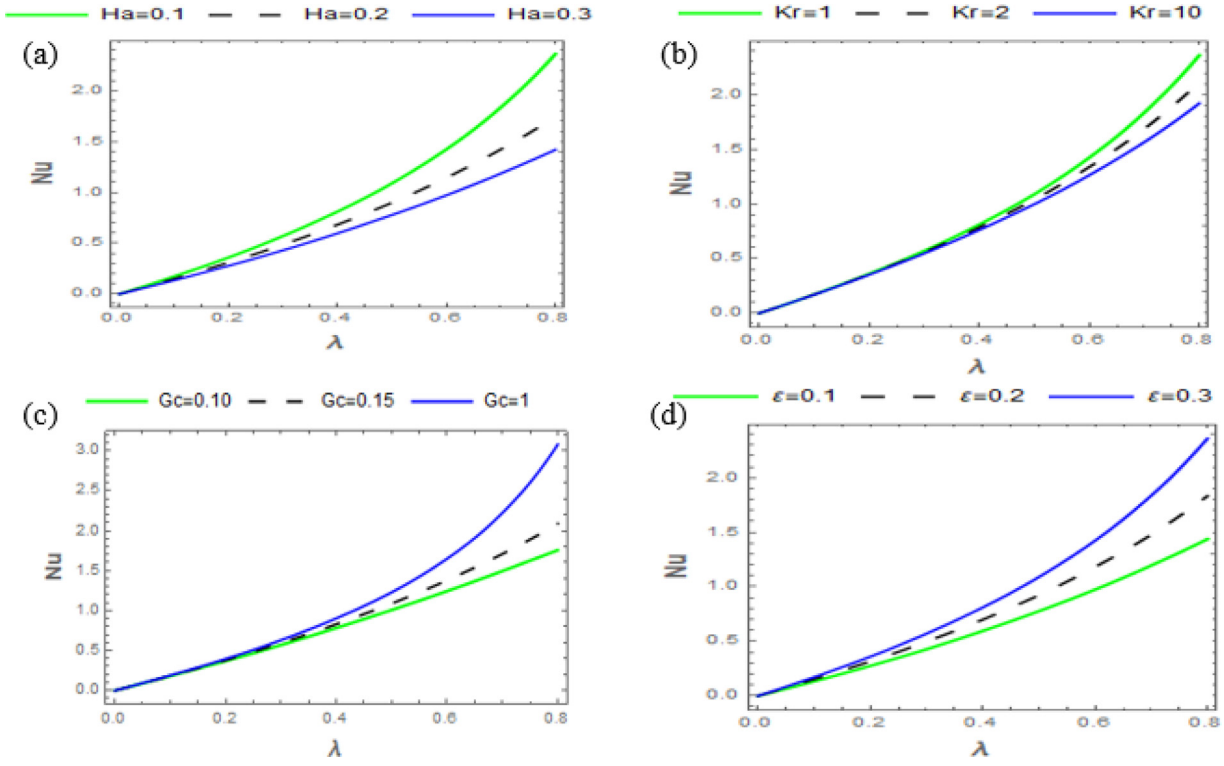

Fig. 8. Inference of Hartmann number (Ha), reactant concentration consumption rate parameter (Kr), concentration buoyancy (Gc), and variable electrical conductivity (ε).

consumption rate parameter (Kr) indicates a reversal of the trend. This is related to the previous explanation. As a result, increasing (decreasing) fluid temperature supports (opposes) the exothermic chemical reactions, which in turn increases (decreases) the heat transfer rate.

5. Conclusion

We have described the magnetohydrodynamics reactive analysis on a steady incompressible flow Featuring Arrhenius energy and exothermic chemical reaction on two vertical plates using a numerical scheme. The key outcomes of the present analysis are highlighted as:

1. The employed method demonstrates an excellent potential in respect to accuracy and convergence for simulating flow
2. Uplifting the magnitude of the magnetic field term is suitable for the reduction of the drag force for exothermic chemical reaction
3. The heat transfer rate upsurges for a rise in the values of Hartmann number, reactant concentration consumption rate while it peters out for concentration buoyancy and variable electrical conductivity.
4. An upsurge in reaction rate parameter, Casson parameter, viscous heating, thermal, and concentration buoyancy parameters, encourages fluid velocity in the channel.
5. The activation energy parameter, reactive strength, concentration buoyancy, and viscous heating propels exothermic chemical reactions of the system.
6. Hartmann number and activation energy parameter, reduce the fluid temperature.

These results from this investigation will help in promoting quality chemical and industrial products. It will as well assist in the appropriate combination and utilization of non-Newtonian Fluid for chemical engineering, thermal sciences, biotechnology, and others. Hence, the analysis can be further considered to explore the case of asymmetric convective heat exchange.

Declaration of competing interest

The authors declare that they have no known competing financial interests or personal relationships that could have appeared to influence the work reported in this paper.

Acknowledgment

The authors appreciate the excellent research facilities provided by kwara state university.

Funding statement

No funding was received for conducting this study.

References

1. Obalalu AM, Ajala OA, Abdulraheem A, Oladimeji AA. The influence of variable electrical conductivity on non-Darcian Casson nanofluid flow with first and second-order slip conditions. *Partial Diff Equ Appl Math*. 2021:100084. http://dx.doi.org/10.1016/j.padiff.2021.100084.
2. Obalalu AM, Ajala AO, Akindele AO, Oladapo OA, Adepoju O, Jimoh OM. Unsteady squeezed flow and heat transfer of dissipative casson fluid using optimal homotopy analysis method: An application of solar radiation. *Partial Diff Equ Appl Math*. 2021:100146. http://dx.doi.org/10.1016/j.padiff.2021.100146.
3. Adesanya S, Oluwadare E, Falade J, Makinde O. Hydromagnetic natural convection flow between vertical parallel plates with time-periodic boundary conditions. *J Magnet Magnet Mater*. 2015;396:295–303.
4. Adesanya SO. Free convective flow of heat generating fluid through a porous vertical channel with velocity slip and temperature jump. *Ain Shams Eng J*. 2015;6(3):1045–1052.
5. Ajala O, Adegbite P, Abimbade S, Obalalu A. Thermal radiation and convective heating on hydro magnetic boundary layer flow of nanofluid past a permeable stretching surface. *Int J Appl Math Stat Sci*. 2019.
6. Makinde OD, Chinyoka T. Numerical investigation of buoyancy effects on hydromagnetic unsteady flow through a porous channel with suction/injection. *J Mech Sci Technol*. 2013;27(5):1557–1568.
7. Noor NaM, Shafie S, Admon MA. Impacts of chemical reaction on squeeze flow of MHD Jeffrey fluid in horizontal porous channel with slip condition. *Phys Scr*. 2021;96(3):035216.
8. Adeosun A, Gbadeyan J, Titiloye E. Heat and mass transfer of a nonlinear convective Arrhenius reactive fluid flow between two vertical plates filled with a porous material. *Eur Phys J Plus*. 2020;135(11):1–17.
9. Hayat T, Waqas M, Shehzad S, Alsaedi A. On 2D stratified flow of an Oldroyd-B fluid with chemical reaction: an application of non-Fourier heat flux theory. *J Mol Liquids*. 2016;223:566–571.
10. Casson N. A flow equation for pigment-oil suspensions of the printing ink type. *Rheol Disperse Syst*. 1959.
11. Obalalu AM. Heat and mass transfer in an unsteady squeezed Casson fluid flow with novel thermophysical properties: Analytical and numerical solution. Heat Transf. http://dx.doi.org/10.1002/htj.22263.
12. Malik M, Naseer M, Nadeem S, Rehman A. The boundary layer flow of casson nanofluid over a vertical exponentially stretching cylinder. *Appl Nanosci*. 2014;4(7):869–873. http://dx.doi.org/10.1007/s13204-013-0267-0.
13. Abolbashari MH, Freidoonimehr N, Nazari F, Rashidi MM. Analytical modeling of entropy generation for casson nano-fluid flow induced by a stretching surface. *J Adv Powder Technol*. 2015;26(2):542–552. http://dx.doi.org/10.1016/j.apt.2015.01.003.
14. Kataria HR, Patel HR. Radiation and chemical reaction effects on MHD Casson fluid flow past an oscillating vertical plate embedded in porous medium. *Alex Eng J*. 2016;55(1):583–595.
15. Makinde OD, Eegunjobi AS. Entropy analysis of thermally radiating magnetohydrodynamic slip flow of casson fluid in a microchannel filled with saturated porous media. *J Porous Media*. 2016;19(9):799–810. http://dx.doi.org/10.1615/JPorMedia.v19.i9.40.
16. Shaw S, Mahanta G, Sibanda PJaEJ. Non-linear thermal convection in a casson fluid flow over a horizontal plate with convective boundary condition. *Alexa Eng J*. 2016;55(2):1295–1304.
17. Raju RS. Unsteady MHD boundary layer flow of casson fluid over an inclined surface embedded in a porous medium with thermal radiation and chemical reaction. *J Nanofluids*. 2018;7(4):694–703. http://dx.doi.org/10.1166/jon.2018.1500.
18. El-Aziz A, Afify AA. MHD Casson fluid flow over a stretching sheet with entropy generation analysis and Hall influence. (6):2019:592. 21, http://dx.doi.org/10.3390/e21060592.
19. Gbadeyan J, Titiloye E, Adeosun A. Effect of variable thermal conductivity and viscosity on Casson nanofluid flow with convective heating and velocity slip. *Heliyon*. 2020;6(1):e03076.
20. Mukhopadhyay S, Vajravelu K, Van Gorder Ra. Casson fluid flow and heat transfer at an exponentially stretching permeable surface. *J Appl Mech Tech Phys*. 2013;80(5).
21. Obalalu AM, Kazeem I, Abdulrazaq A, Ajala OA, Oluwaseyi A, Adeosun AT, Adebayo LL, Wahaab FA. Numerical simulation of entropy generation for casson fluid flow through permeable walls and convective heating with thermal radiation effect. *J Serbian Soc Comput Mech*. 2020;14(2):503–519. http://dx.doi.org/10.24874/jsscm.2020.14.02.10.
22. Obalalu AM, Ajala OA, Adeosun AT, Wahaab FA, Oluwaseyi A, Adebayo LL. Natural convective non-Newtonian Casson fluid flow in a porous medium with slip and temperature jump boundary conditions. *Petrol Coal*. 2020;62(4):1532–1545.
23. Waqas M. A mathematical and computational framework for heat transfer analysis of ferromagnetic non-Newtonian liquid subjected to heterogeneous and homogeneous reactions. *Magnet Mater*. 2020;493:165646.
24. Wahaab FA, Adebayo LL, Rostami A, Ganeson M, Yusuf JY, Afeez Y, Obalalu AM, Abdulraheem A, Oladosu TL. Microwave absorption performance of Ni 0.5 Zn 0.5 Fe2O4 nanoclusters at 8.2–18 GHz frequency. *Indian J Phys*. 2021:1–11. http://dx.doi.org/10.1007/s12648-021-02005-4.
25. Ajala Obalalu, Abimbade, Akinyemi. Numerical study of forced convective heat generation flow through a permeable walls with Suction/injection. *Int J Sci Res Publ*. 2019;9(6).
26. Ajala Adegbite, Abimbade, Obalalu. Thermal radiation and convective heating on hydromagnetic boundary layer flow of nanofluid past a permeable stretching surface. *Int J Appl Math Stat Sci (IJAMSS)*. 2019;2(8).
27. Hartmann J, Lazarus F. Hg-dynamics II. Theory of laminar flow of electrically conductive liquids in a homogeneous magnetic field. 1937;15(7).
28. Obalalu AM, Wahaab FA, Adebayo LL. Heat transfer in an unsteady vertical porous channel with injection/suction in the presence of heat generation. *J Taibah Univ Sci*. 2020;14(1):541–548. http://dx.doi.org/10.1080/16583655.2020.1748844.
29. Abbas SZ, Khan WA, Kadry S, Khan MI, Waqas M, Khan MI. Entropy optimized Darcy-Forchheimer nanofluid (silicon dioxide, molybdenum disulfide) subject to temperature dependent viscosity. *Comput Methods Progr Biomed*. 2020;190:105363.
30. Obalalu AM, Wahaab FA, Adebayo LL. Heat transfer in an unsteady vertical porous channel with injection/su ction in the presence of heat generation. *J Taibah Univ Sci*. 2020;14(1):541–548.

31. Gopal D, Saleem S, Jagadha S, Ahmad F, Almatroud AO, Kishan N. Numerical analysis of higher order chemical reaction on electrically MHD nanofluid under influence of viscous dissipation. *Alex Eng J*. 2021;60(1):1861–1871. http://dx.doi.org/10.1016/j.aej.2020.11.034.
32. Eegunjobi A, Makinde O. Entropy generation analysis in a variable viscosity MHD channel flow with permeable walls and convective heating. *Math Probl Eng*. 2013;2013.
33. Waqas M. Simulation of revised nanofluid model in the stagnation region of cross fluid by expanding-contracting cylinder. *Int J Numer Methods Heat Fluid Flow*. 2019.
34. Hayat T, Qayyum S, Alsaedi A. Thermally radiative stagnation point flow of maxwell nanofluid due to unsteady convectively heated stretched surface. *J Molecular Liquids*. 2016;224:801–810.